

**NANOPARTICLES OF TUNGSTEN AS LOW-COST MONOMETALLIC CATALYST FOR SELECTIVE HYDROGENATION OF 3-HEXYNE****María Juliana Maccarrone<sup>a,\*</sup>, Cecilia Lederhos<sup>a</sup>, Carolina Betti<sup>a</sup>, Nicolás Carrara<sup>a</sup>, Juan C. Yori<sup>a,b</sup>, Fernando Coloma Pascual<sup>c</sup>, Domingo Liprandi<sup>a,b</sup>, Carlos Vera<sup>a,b</sup> and Mónica Quiroga<sup>a,b</sup>**<sup>a</sup>Instituto de Investigaciones en Catálisis y Petroquímica INCAPE (FIQ-UNL, CONICET), Predio CCT CONICET Santa Fe, Colectora Ruta Nac. N° 168 Km 0 - Paraje El Pozo, (3000) Santa Fe, Argentina<sup>b</sup>Facultad de Ingeniería Química, Universidad Nacional del Litoral, Santiago del Estero 2829, S3000AOJ Santa Fe, Argentina<sup>c</sup>Facultad de Ciencias, Universidad de Alicante, Apartado 99, E-03080 Alicante, Spain

Recebido em 24/04/2015; aceito em 08/09/2015; publicado na web em 11/11/2015

Low-cost tungsten monometallic catalysts containing variable amounts of metal (4.5, 7.1 and 8.5%W) were prepared by impregnating alumina with ammonium metatungstate as an inexpensive precursor. The catalysts were characterized using ICP, XPS, XRD, TPR and hydrogen chemisorption. These techniques revealed mainly  $WO_3-Al_2O_3$  ( $W^{6+}$ ) species on the surface. The effects of the content of W nanoparticles and reaction temperature on activity and selectivity for the partial hydrogenation of 3-hexyne, a non-terminal alkyne, were assessed under moderate conditions of temperature and pressure. The monometallic catalysts prepared were found to be active and stereoselective for the production of (*Z*)-3-hexene, had the following order: 7.1WN/A > 8.5 WN/A ≥ 4.5 WN/A. Additionally, the performance of the synthesized xWN/A catalysts exhibited high sensitivity to temperature variation. In all cases, the maximum 3-hexyne total conversion and selectivity was achieved at 323 K. The performance of the catalysts was considered to be a consequence of two phenomena: a) the electronic effects, related to the high charge of W (+6), causing an intensive dipole moment in the hydrogen molecule (van der Waals forces) and leading to heterolytic bond rupture; the  $H^+$  and  $H^-$  species generated approach a 3-hexyne adsorbate molecule and cause heterolytic rupture of the  $C\equiv C$  bond into  $C=C^+$ ; and b) steric effects related to the high concentration of  $WO_3$  on 8.5WN/A that block the  $Al_2O_3$  support. Catalyst deactivation was detected, starting at about 50 min of reaction time. Electrodeficient  $W^{6+}$  species are responsible for the formation of green oil at the surface level, blocking pores and active sites of the catalyst, particularly at low reaction temperatures (293 and 303 K). The resulting best catalyst, 7.1WN/A, has low fabrication cost and high selectivity for (*Z*)-3-hexene (94%) at 323 K. This selectivity is comparable to that of the classical and more expensive industrial Lindlar catalyst (5 wt% Pd). The alumina supported tungsten catalysts are low-cost potential replacements for the Lindlar industrial catalyst. These catalysts could also be used for preparing bimetallic W-Pd catalysts for selective hydrogenation of terminal and non-terminal alkynes.

Keywords: tungsten; monometallic catalyst; selective hydrogenation; non-terminal alkyne.

**INTRODUCTION**

The selective hydrogenation of alkynes via heterogeneous catalysis for obtaining the (*Z*) or (*E*)-alkenes has multiple applications in fine chemistry, for the pharmacy, agrochemical and petrochemical industries. Particularly the production of (*Z*)-alkenes is a reaction of central relevance in the production of bioactive molecules, natural products and flavors.<sup>1-3</sup> This kind of reactions is also crucial during the process of fabrication of polymers, for the complete elimination of alkyne impurities present in the alkene feeds to the reactor, as alkyne traces greatly decrease the quality of the obtained polymers,<sup>4</sup> poisoning the polymerization catalysts.<sup>1,4</sup>

The heterogeneous catalysts based on Pd that are commonly used in these reactions have some problems because of their high hydrogenation activity. They over reduce the alkenes to alkanes or produce isomerization, in any case decreasing the yield of the desired products. The most widely used catalyst for this kind of reactions, for obtaining alkenes in (*Z*) configuration, is the classical Lindlar catalyst, introduced as early as 1953. This is made supporting about 5 wt% Pd over  $CaCO_3$  promoting it with lead-compounds such as  $Pb(OAc)_2$  in amounts of 2-3 wt%.<sup>5</sup> For decades the research on selective hydrogenation was focused on modifying the properties of the Lindlar catalyst in order to increase the activity and selectivity

to alkenes of short chain length. However the catalysts suffer from limited reuse, deactivation, presence of toxic Pb, a need for the injection of inconveniently high amounts of amine, etc. Moreover there is still a lack of knowledge on the nature of the active sites.<sup>6</sup> Due to the high cost of the Lindlar catalyst and its mentioned disadvantages the development of heterogeneous catalysts of lower cost, high activity, selectivity and stability, has been a challenge during many years for the researchers of the field.

Supported nickel is perhaps the most used metal catalyst having both a good activity level and a fairly low cost. For some reactions however its selectivity is low and the activity level quite low, demanding high temperatures and pressures for running the reaction with appropriate yields. Another fairly cheap metal catalyst is supported tungsten, that has proved to be an efficient catalyst in many processes of petrochemical interest, or for allylation of aldehydes under solvent free conditions,<sup>7</sup> or for butanol dehydration.<sup>8</sup> However its use for selective hydrogenations is less known. In previous reports of the group, results on the alternative use of Ni monometallic catalysts (3.5 wt% Ni, using  $NiCl_2$  as precursor salt) and W monometallic catalysts (2.4 wt% W, with  $H_3PO_4 \cdot 12WO_3$  as an acidic precursor), supported over  $\gamma$ -alumina, were disclosed.<sup>9,10</sup> The reports were focused on the activity, selectivity and reaction kinetics for the selective hydrogenation at mild reaction conditions of 1-heptyne, a terminal alkyne of medium chain length. A total conversion of about 98% and a selectivity to 1-heptene of 75% was obtained at 323 K, 1.5 bar and

\*e-mail: jmaccarrone@fiq.unl.edu.ar

150 min reaction time, for molar ratios of reactant-to-metal of 64 and 294 when active sites were Ni or W, respectively. The kinetic studies indicated that the rate limiting step for both catalysts was the dissociative adsorption of hydrogen. In these contributions it was reported that when using tungsten based catalyst, important variations in the activity and selectivity were obtained when the pretreatment or the reaction temperature were changed.

On the other hand, there are scarce reports that deal with the partial hydrogenation of medium chain non-terminal alkynes.<sup>11-13</sup> Particularly in the open literature, the selective hydrogenation of 3-hexyne has been relatively less studied and mainly using noble metal based monometallic, bimetallic or supported complexes as catalysts.<sup>11,14-17</sup> The effect of the temperature on the selectivity to the (*Z*) isomers during the selective hydrogenation of non-terminal alkynes is particularly not clear. An example of the effect of the reaction temperature is the paper by Choi and Yoon, who found that the selectivity to the (*Z*)-alkene over a Ni catalyst was increased when the temperature was decreased.<sup>18</sup> In a previous contributions of our group different low-loaded Pd bimetallic catalysts supported on  $\gamma$ -alumina (W–Pd/Al<sub>2</sub>O<sub>3</sub> and Pd–Ni/Al<sub>2</sub>O<sub>3</sub>) were tested for the partial hydrogenation of 3-hexyne. A little effect of the reaction temperature (from 273 to 323 K) on the selectivity to the (*Z*)-3-hexene (ca. 93%) was found.<sup>15</sup> Also in the case of Pd(II) and Rh(I) complexes anchored on alumina or a carbonaceous support a low sensitivity of the selectivity to temperature variations was found.<sup>16,17</sup>

In this context the objectives of this work are: a) to prepare a low-cost W monometallic catalyst supported on  $\gamma$ -alumina; b) to evaluate the effect of the tungsten loading; and c) to study the effect of the reaction temperature at moderate hydrogen pressure on the activity and selectivity during the partial hydrogenation of 3-hexyne, a medium-chain non-terminal alkyne.

## EXPERIMENTAL

### Catalyst preparation

Monometallic tungsten catalysts supported on alumina were prepared using an ammonium precursor salt by the incipient wetness technique.  $\gamma$ -Al<sub>2</sub>O<sub>3</sub> Ketjen CK 300 ( $S_{\text{BET}}$ : 180 m<sup>2</sup> g<sup>-1</sup>) previously calcined in air at 823 K during 4 h was used as support. The volume and concentration of the impregnating solutions were adjusted to obtain 4.5, 7.1 and 8.5 wt% of W on the final catalysts. Solutions of variable W content were prepared at pH=1 using (NH<sub>4</sub>)<sub>6</sub>H<sub>2</sub>W<sub>12</sub>O<sub>40</sub>·xH<sub>2</sub>O (Aldrich, Cat No.463922) as the precursor salt to get monometallic catalysts. These were named xWN/A. After impregnation, the catalysts were dried overnight at 373 K and calcined in an air flow at 823 K during 3 h. Before each run the catalysts were reduced in a hydrogen stream (105 mL min<sup>-1</sup>, 673 K) for 1 h.

The commercial Lindlar catalyst was provided by Aldrich (5 wt% Pd, Cat. No. 20,573-7) and was used without any previous pretreatment, as suggested by several authors studying alkyne selective hydrogenation reactions, for comparative purposes.<sup>19</sup>

### Catalyst characterization

The tungsten metal loading of the catalysts was determined by digesting the samples and then analyzing the liquors by inductively coupled plasma analysis (ICP) in an OPTIMA 2100 DV Perkin Elmer equipment.

The hydrogen chemisorption of the metal particles on the catalysts surface was measured at 373 K in a Micromeritics AutoChem II 2920 instrument equipped with a thermal conductivity detector (TCD). 0.2 g of the samples were reduced *in situ* in a 5% (v/v) hydrogen/argon

stream during 1 h at 673 K. The samples were degassed *in situ* in an argon flow (AGA, 99.99%) and cooled down to 373 K. Then the hydrogen uptake was measured by sending calibrated pulses.

The reducibility of the surface species was determined by Temperature Programmed Reduction (TPR), using a Micromeritics AutoChem II instrument equipped with a thermal conductivity detector. Before the TPR tests the samples were dried *in situ* at 673 K for 30 min in an oxygen flow (AGA purity 99.99%). After that, the samples were cooled down to 298 K in an argon flow. Then the temperature was increased up to 1223 K at 10 K min<sup>-1</sup> in a H<sub>2</sub>/Ar (5% v/v) gas flow.

X-ray diffractograms (XRD) of powdered samples were obtained using a Shimadzu XD-D1 instrument with CuK $\alpha$  radiation ( $\lambda = 1.5405 \text{ \AA}$ ) in the 21° < 2 $\theta$  < 49° range and at a scan speed of 0.25° min<sup>-1</sup>. Samples were powdered and reduced *ex situ* in hydrogen, then they were immediately put in the chamber of the equipment and the test was initiated.

The electronic states of the surfaces species were determined by X-ray Photoelectron Spectroscopy (XPS) in a VG-Microtech Multilab equipment, equipped with a MgK $\alpha$  (hv: 1253.6 eV) radiation and a pass energy of 50 eV. The analysis pressure during data acquisition was 5.10<sup>-7</sup> Pa. Samples were treated *in situ* with a H<sub>2</sub> stream following the same pretreatment conditions for each catalyst. A careful deconvolution of the spectra was made and the areas under the peaks were estimated by calculating the integral of each peak after subtracting a Shirley background and fitting the experimental peak to a combination of Lorentzian / Gaussian lines of 30 / 70% proportions. The reference binding energy (BE) was Al 2p line at 74.4 eV. For quantification, the areas were normalized using the sensitivity factors of each element.

### Catalytic evaluations

Catalytic reaction tests were carried out in a stainless steel (completely coated with PTFE) stirred tank batch reactor equipped with a magnetically coupled stirrer with two blades in counter-rotation operated at 800 rpm. The reactant 3-hexyne (Fluka, Cat. No. 51950, purity > 98%) was dissolved to a 2% (v/v) in toluene (Merck, Cat. No. TX0735-44, purity > 99%). The tests were performed using the following conditions: 1.5 bar hydrogen pressure, 293 to 323 K reaction temperature, 0.3 g of a 60–120 mesh catalyst particle size and 200 min reaction time. The commercial Lindlar catalyst was used as a reference at identical operational conditions of temperature, pressure and initial concentration of 3-hexyne (with a molar ratio alkyne/Pd = 1115).

In order to eliminate external diffusional limitations the runs were carried out using different stirring speeds in the range of 180-1400 rpm. It was found that external gas-liquid limitations were absent at stirring rates higher than 500 rpm. On the other hand, in order to ensure that catalytic results were not influenced by intraparticle mass transfer limitations, the catalyst pellets were milled to samples of different particle size: pellets of 1500  $\mu\text{m}$  (not milled), a fraction between 60-100 mesh (250-150  $\mu\text{m}$ ) and a fraction bigger than 100 mesh (<150  $\mu\text{m}$ ). The obtained values of 3-hexyne conversion were the same for the two milled fractions indicating the absence of internal diffusional limitations. Thus a stirring rate of 800 rpm and particles smaller than 250  $\mu\text{m}$  were used in all the tests.

Catalytic evaluations were carried out in duplicates with an experimental error lower than 5%. Reactants and products were analyzed by gas chromatography using a flame ionization detector and a GS-GAS PRO capillary column (60 m long, 0.32 mm ID). In order to identify each possible reaction product, pure chromatographic patrons of 3-hexyne, (*Z*)-3-hexene, (*E*)-3-hexene, (*Z*)-2-hexene,

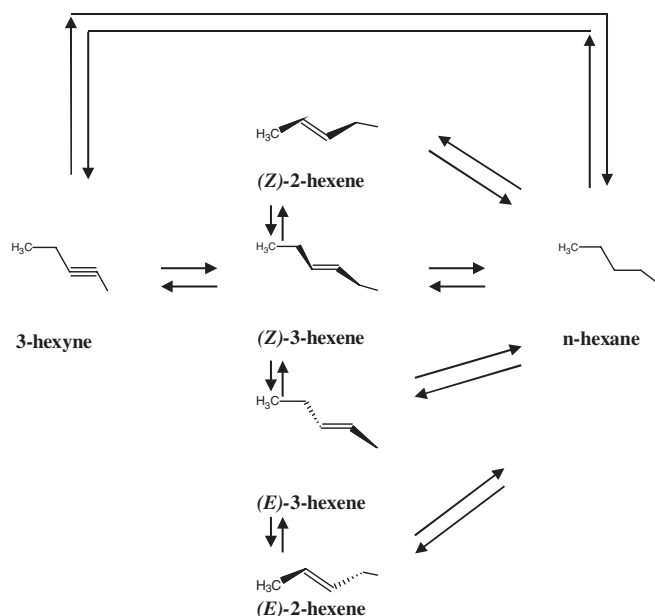


Figure 1. Scheme of the 3-hexyne reversible hydrogenation reactions

(*E*)-2-hexene and n-hexane were injected according with the reaction network proposed by Alvez-Manoli *et al.* presented in Figure 1.<sup>14</sup>

In order to compare the performance of the catalysts, the initial reaction rate of 3-hexyne was calculated using the following formula:

$$r_A^0 = \frac{V \cdot C_A^0}{W_{\text{cat}}} \cdot \left( \frac{\partial X_A}{\partial t} \right)_{t=0} \quad \text{Eq. (1)}$$

where:  $r_A^0$ : initial reaction rate of 3-hexyne [ $\text{mol g}_{\text{cat}}^{-1} \text{h}^{-1}$ ];  $\left( \frac{\partial X_A}{\partial t} \right)_{t=0}$ : tangent value of the 3-hexyne total conversion vs. time curve at  $t=0$ ;  $C_A^0$ : initial concentration of 3-hexyne [ $\text{mol L}^{-1}$ ];  $W_{\text{cat}}$ : catalyst mass [g];  $V$ : reaction volume [L];  $t$ : reaction time [h].

## RESULTS AND DISCUSSION

### Catalyst characterization

The results of the chemical analysis as obtained by ICP confirmed the metal loading of each catalyst; within a 5% error, which was considered negligible. These values are presented in Table 1. For the monometallic tungsten catalysts no consumption of hydrogen was detected during the chemisorption analysis indicating that at the evaluated conditions there are no surface sites capable of adsorbing hydrogen, in accord with previously reported results for monometallic tungsten-alumina materials.<sup>10,15,20-22</sup>

Table 1. Metal Loading (ICP), binding energies (BE) for W 4f<sub>7/2</sub> and W/Al atomic ratios (XPS)

Catalysts	Metallic W (w %)	XPS	
		BE (eV)	Atomic Ratios
		W 4f <sub>7/2</sub>	W/Al
4.5WN/A	4.5	36.08	0.016
7.1WN/A	7.1	36.07	0.024
8.5WN/A	8.5	36.05	0.027

The TPR traces of the xWN/A samples are plotted in Figure 2. The obtained TPR profile of the catalysts are quite similar, presenting

a small reduction peak at ca. 1155 K, with a maximum hydrogen consumption at temperatures higher than 1200 K. For W loadings below the monolayer value (as it is our case) there would be only WO<sub>x</sub> tetrahedra species with a strong interaction with the support and this interaction would have a marked influence on the reduction pattern.<sup>22-25</sup> For this reason the reducibility of tungsten supported on alumina is more difficult when the tungsten loading is low.<sup>25</sup> Besides, the TPR profile of 8.5WN/A sample additionally has a peak at 797.9 K, that could be related to the reduction in several steps of octahedrally coordinated WO<sub>x</sub> species.<sup>25,26</sup>

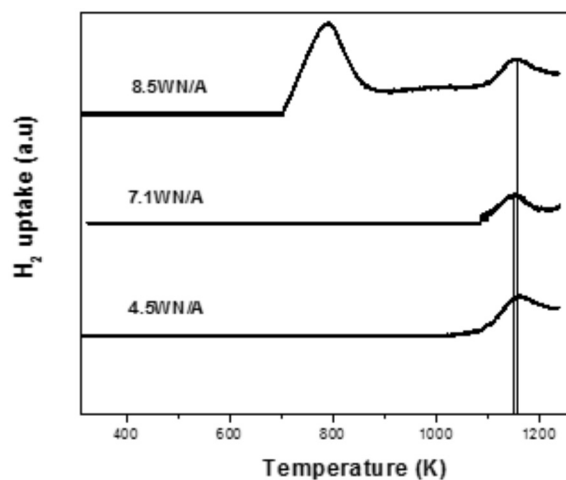


Figure 2. Temperature programmed reduction traces of the xWN/A catalysts

The diffractograms of the catalysts obtained by XRD measurements are identical. Figure 3 shows the diffractogram of sample 8.5WN/A that only the typical signals characteristic of the gamma phase of alumina: 37.7°, 45.98° and 66.98°.<sup>27,28</sup> The absence of peaks in the 20° < 2θ < 30° region indicates that there are no tungsten oxides present as a crystalline segregated phase. According to the bibliography WO<sub>3</sub> crystallites can be detected by XRD only when W loading are higher than ca. 20%.<sup>22,25,29</sup> This is equivalent to W surface concentrations higher than the corresponding monolayer value (4.3 W atoms nm<sup>-2</sup>),<sup>30</sup> therefore due to the low W loading used in our case, 4.5 to 8.5 wt% W, far below the detection limit of the equipment used, the presence of crystalline species was not detected by XRD.<sup>22,25</sup>

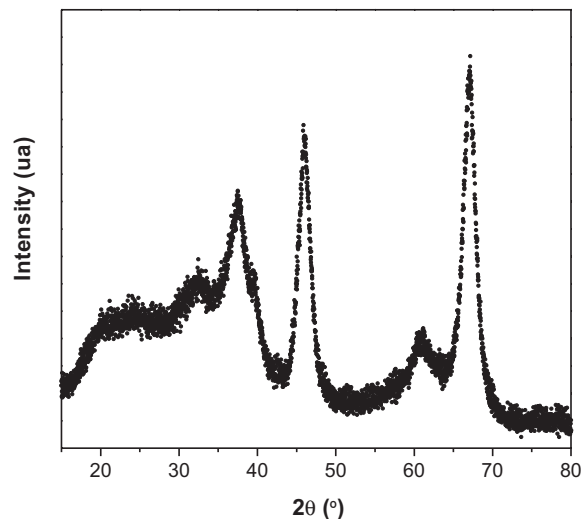


Figure 3. XRD diffractogram of 8.5WN/A catalyst

The XPS spectra of W  $4f_{7/2}$  for the xWN/A catalysts are shown in Figure 4. The spectra of the three catalysts with different metal loadings are quite similar. In Table 1 the maximum binding energies (BE) of the W  $4f_{7/2}$  peaks and the W/Al atomic ratios were also reported. According to the literature the BE of W  $4f_{7/2}$  in the case of metallic tungsten ( $W^0$ ) appears at 34.0 eV.<sup>31</sup>

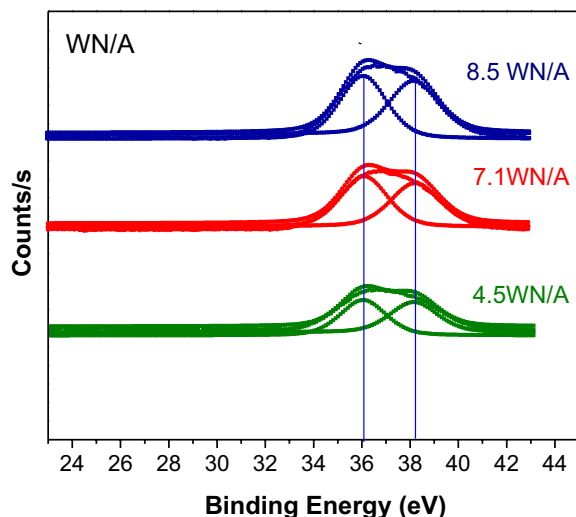


Figure 4. XPS spectra of the W  $4f_{7/2}$  region for WN/A catalysts

The xWN/A monometallic catalysts reduced at 673 K presented very similar BE ca. 36.07 eV. These BE values indicate the presence of  $WO_x$  species with  $W^{6+}$  on the catalysts surface after calcination and reduction.<sup>25,31-34</sup> The atomic ratios of W/Al by XPS shown in Table 1, indicate an increasing content of tungsten at the surface as the metal loadings of the catalysts is increased.

At the pretreatment conditions used during the preparation of the catalysts, the TPR and XPS analysis suggest the presence of tetrahedral  $WO_3 - Al_2O_3$  ( $W^{+6}$ ) species, on the xWN/A catalysts. TPR also suggests the presence of octahedral  $WO_x$  species on the 8.5WN/A catalyst. Because of the low W loading, far below the detection limit of the equipment used, no segregated crystalline species were detected by XRD.

### Catalytic tests

Results of 3-hexyne total conversion as a function of time and temperature are presented in Figures 5a to 5c for the tungsten monometallic catalysts 4.5WN/A, 7.1WN/A and 8.5WN/A, respectively. In these figures it can be seen that all the prepared monometallic tungsten catalysts are active in the evaluated temperature range, even at the lowest temperature, 293 K. Although the hydrogenation reactions are exothermic, for the three W loadings the highest conversion of 3-hexyne was obtained at the highest temperature used, 323 K, suggesting that the system is dominated by kinetic effects rather than thermodynamic. Also, it can be deduced from Figures 5 that independent of the reaction temperature used, the 7.1WN/A is the catalyst with the highest activity for the conversion of 3-hexyne. In Figure 5 it can be noted that after 50 minutes on-stream, for all the catalytic systems there is a change of the 3-hexyne reaction rate. This fact can be related to equilibrium saturation of the surface or to a deactivation process.

Figure 6 shows the total conversion of 3-hexyne as a function of time, at three different temperatures, for the commercial Lindlar catalyst. It can be seen that for the reference catalyst the 3-hexyne conversion plots are very similar at the highest temperatures used (303 and 323 K).

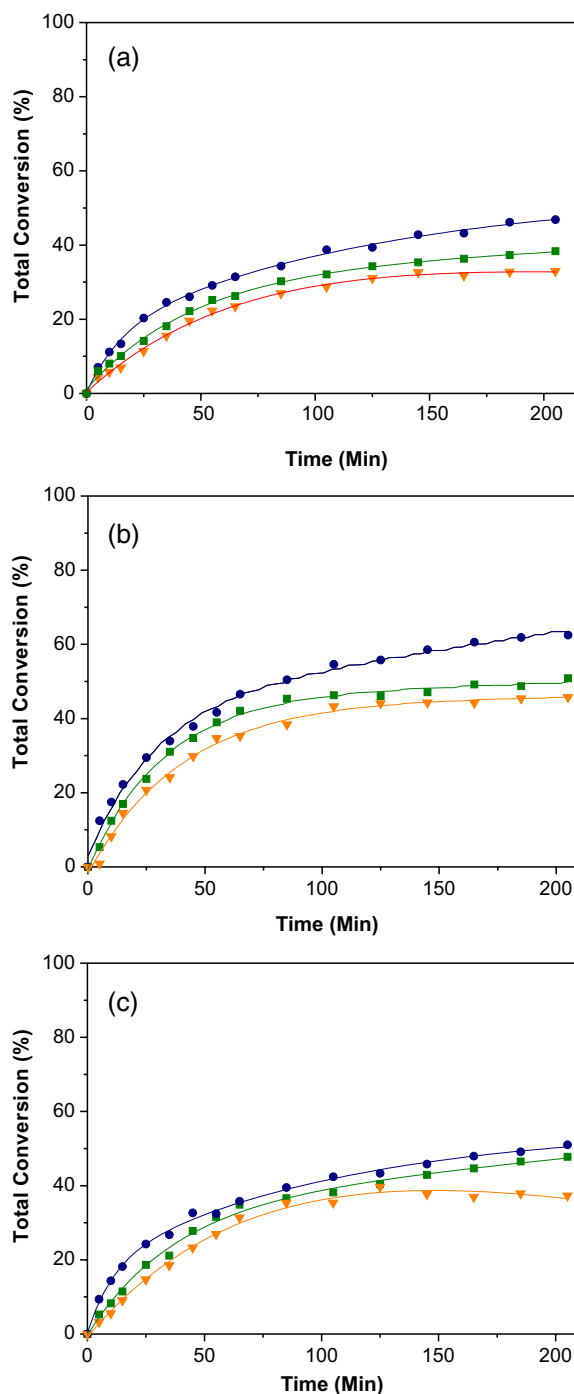
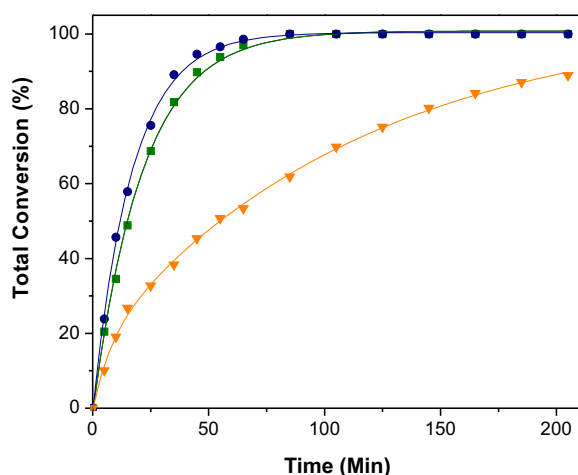


Figure 5. 3-hexyne total conversion (%) as a function of time for a) 4.5WN/A, b) 7.1WN/A and c) 8.5WN/A catalysts evaluated at 1.5 bar and different temperatures:  $T_1 = 293$  K ( $\nabla$ ),  $T_2 = 303$  K ( $\blacksquare$ ) and  $T_3 = 323$  K ( $\bullet$ )

Initial reaction rates ( $r_A^0$ ) and values of selectivity to the (*Z*)-3-hexene, (*E*)-3-hexene and n-hexane are presented in Tables 2 and 3.

Inspection of the values of Table 2 shows that for all the catalytic systems the initial reaction rates increased with the temperature. At all temperatures the most active catalyst was 7.1WN/A. It also has the highest  $r_A^0$  at 323 K.

Figure 7 shows the values of selectivity to the isomers (*Z*) and (*E*)-3-hexene at different reaction temperatures. In Table 3 and Figure 7 it can be seen that for all the catalytic systems the selectivity to the (*Z*) isomers increased at higher temperatures. With respect to the selectivity to (*Z*)-3-hexene obtained on different catalysts at each temperature, the order found was: 7.1WN/A > 8.5WN/A > 4.5WN/A.



**Figure 6.** 3-hexyne total conversion (%) as a function of time for Lindlar catalyst evaluated at 1.5 bar and different temperatures:  $T_1 = 293\text{ K}$  ( $\blacktriangledown$ ),  $T_2 = 303\text{ K}$  ( $\blacksquare$ ) and  $T_3 = 323\text{ K}$  ( $\bullet$ )<sup>44</sup>

**Table 2.** Initial 3-hexyne reaction rate ( $r_A^0$ ) at different temperatures; 1.5 bar and 800 rpm

Catalysts	$r_A^0$ ( $\text{mol}_A \text{ g}_{\text{cat}}^{-1} \text{ h}^{-1}$ )		
	293 K	303 K	323 K
4.5WN/A	0.019	0.020	0.024
7.1WN/A	0.021	0.029	0.042
8.5WN/A	0.012	0.019	0.034

**Table 3.** Selectivity to (Z)-3-hexene, (E)-3-hexene or n-hexane at different temperatures

Catalysts	293K			303K			323K		
	(Z)	(E)	n	(Z)	(E)	n	(Z)	(E)	n
4.5WN/A	64	20	16	70	19	11	87	10	3
7.1WN/A	66	21	13	75	17	8	94	5	1
8.5WN/A	64	24	12	71	21	8	92	7	1
Lindlar <sup>a</sup>	98	1.7	0.3	98	1.4	0.6	97	2	1

<sup>a</sup>from Ref. 15.

For 7.1WN/A catalyst at 323 K the selectivity to the desired product was the highest (ca. 94%) being comparable to that obtained with the Lindlar catalyst (see Figure 7).

The performance of the catalysts can be interpreted in terms of I) electronic effects, related to the high charge of W. While the low activity of 8.5WN/A catalyst is related to II) a steric effect related to the presence of octahedral  $\text{WO}_3$ , that blocks the  $\text{Al}_2\text{O}_3$  support. Conceptual brief descriptions for each of them are presented in Figures 8 and 9, and are explained below.

#### I) Electronic Effects (Catalytic Cycle):

$\text{WO}_3$  (with  $\text{W}^{6+}$ ) is the active site that facilitates the reaction between  $\text{H}_2$  and 3-hexyne, during the catalytic cycle, which can be seen in Figure 8, with the following consecutive steps:

- 1) The high electron deficiency of tungsten ( $\text{W}^{6+}$ ) provokes firstly, due to van der Waals forces, an intense dipole moment in the hydrogen molecule conducting to a heterolytic bond rupture into  $\text{H}^-$  and  $\text{H}^+$ .

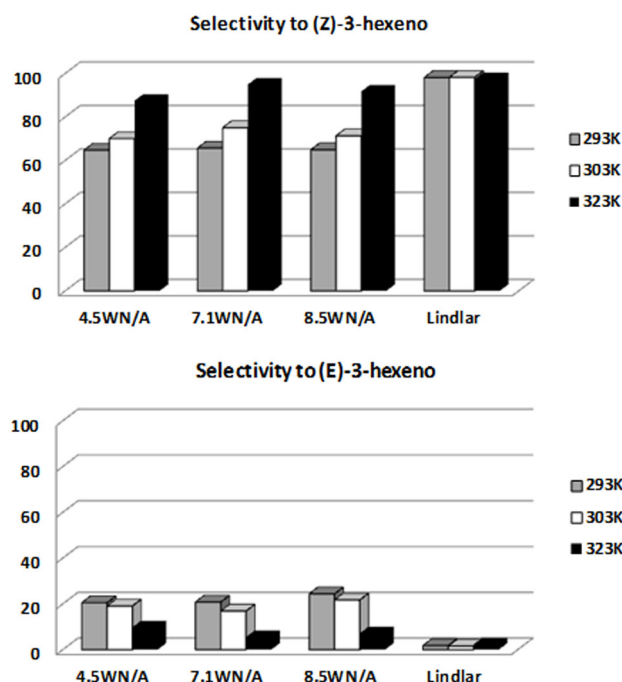


**Figure 7.** Selectivities to (Z)-3-hexene and (E)-3-hexene for  $x\text{WN/A}$  and Lindlar catalysts at different temperatures:  $T_1 = 293\text{ K}$ ,  $T_2 = 303\text{ K}$  and  $T_3 = 323\text{ K}$

- 2) Both species,  $\text{H}^-$  and  $\text{H}^+$ , in turn when approaching to the 3-hexyne alumina adsorbed molecule, provokes the heterolytic rupture of the  $\text{C} \equiv \text{C}$  into  $\text{C}^+ = \text{C}^-$ ,
- 3) and simultaneously,  $\text{H}^-$ ,  $\text{H}^+$  and  $\text{C}^+ = \text{C}^-$  interact to form new bonds generating the desired product, the (Z)-3-hexene molecule.
- 4) On the other hand, due to the presence of 3-hexyne, the (Z)-alkene is desorbed while the alkyne is chemisorbed, as the alkyne (2  $\pi$  bonds) is more strongly adsorbed than the alkene (1  $\pi$  bond).

#### II) Steric Effects

The alumina support promotes the chemisorption of the alkyne due to physical-chemical interactions. In our heterogeneous systems the presence of the support provides a higher concentration of the substrate on catalyst active sites. On the other hand, the high electronegativity of oxygen in the  $\text{WO}_3$  phase does not favor the chemisorption of 3-hexyne. In Figure 9 is shown that, when the concentration of W is too high, 8.5 WN/A sample, there would be less alumina surface free to chemisorb the substrate, and so the rate of hydrogenation considerably fell down.

On the other hand, although all the prepared tungsten monometallic catalysts were active in the studied temperature range, a reduction of the reaction rate of 3-hexyne is noted for all the catalytic systems from 50 min, (see Figure 5). The 7.1WN/A catalyst operated at 323 K was the most stable one, keeping a high conversion for a longer time, in comparison to the other tested catalysts. Some authors have reported that in the case of alkyne reaction the causes of catalyst deactivation are poisoning and fouling of the active sites.<sup>35</sup> In the case of the poisoning of the catalyst this is due to the strong reversible or irreversible adsorption of a molecule that blocks the site for the adsorption and reaction of the main reactants.<sup>36</sup> The fouling is a typical effect appearing when reacting hydrocarbons and it is related to the transformation of the main reactants into undesired species that become strongly adsorbed on the active sites, blocking them for the main reaction.<sup>37</sup> Usually they are carbonaceous oligomers or polymers, termed “green-oil” in the case of the reactions of alkynes. They modify the catalytic performance by changing the

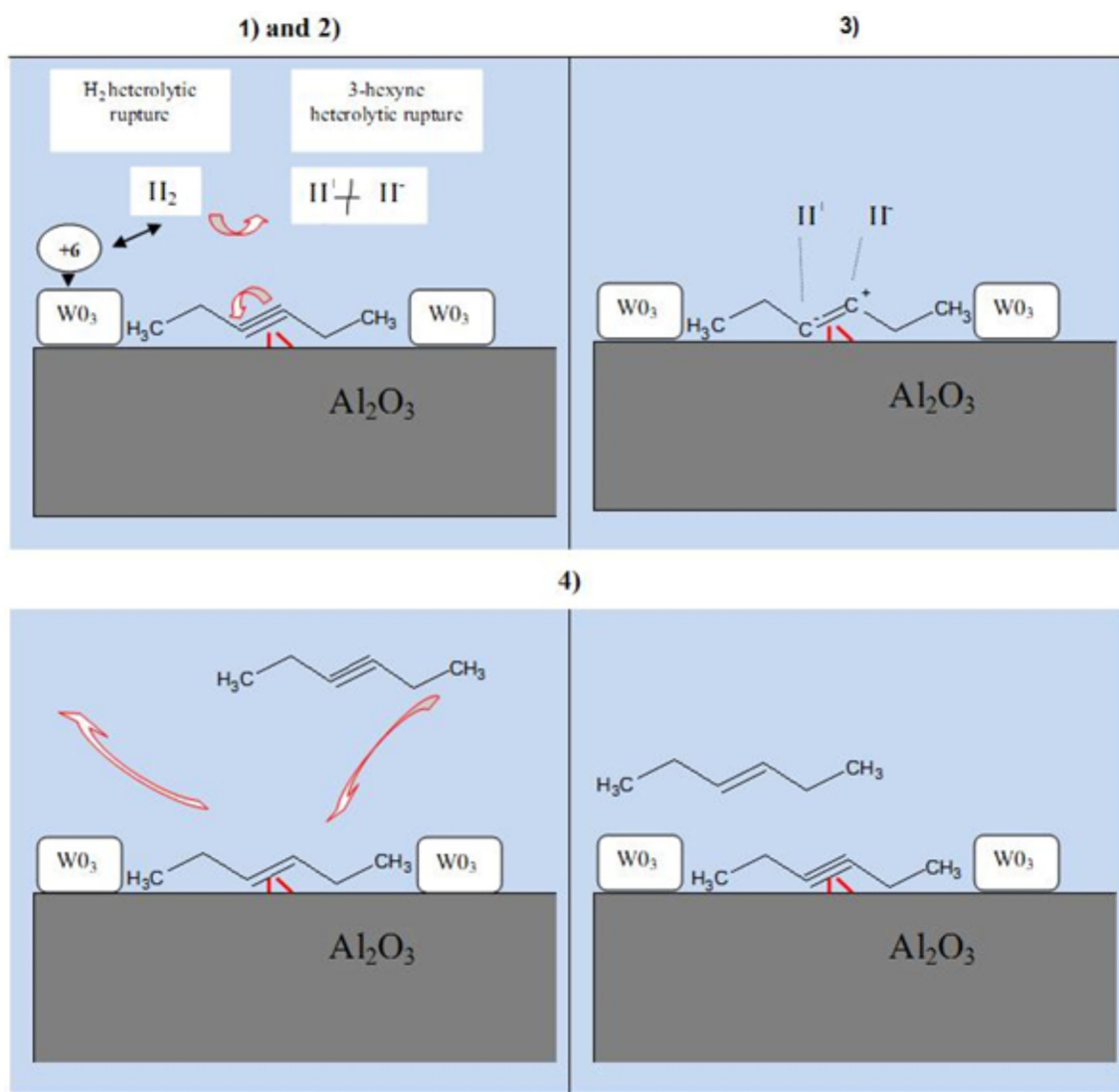


**Figure 8.** Scheme of the Electronic Effects. Steps: 1)  $\text{H}_2$  heterolytic rupture, 2) 3-hexyne heterolytic rupture, 3) Formation of  $(Z)$ -3-hexene and 4) desorption of  $(Z)$ -3-hexene

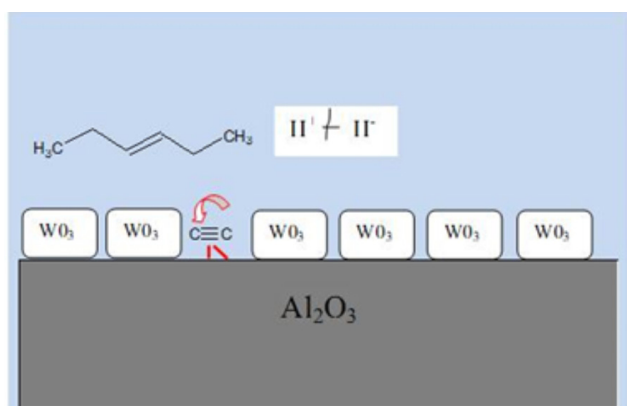


**Figure 9.** Scheme of Steric Effects

surface properties, reducing the available surface area, poisoning the active sites and limiting the diffusion of the alkyne into the catalyst.<sup>4,38-43</sup> For these reasons deactivation is one of the main challenges for the successful design and operation of catalytic processes. The structure and nature of the catalyst support is sometimes related to the deactivation process. Some supports have acid sites capable

of catalyzing the oligomerization of molecules of the feed and the deactivation rate is proportional to the concentration of these acid sites.<sup>44-48</sup> In contrast some authors report that there exists a drastic deactivation when the acid sites disappear.<sup>49,50</sup> Others have found that the concentration of acid sites is not affected by severe coking and loss of activity.<sup>51</sup> In a recent work Esmaili *et al.*<sup>52</sup> studied an alumina supported catalyst for acetylene hydrogenation and found that the presence of more unsaturated constituents and the formation of more branched hydrocarbons were responsible for the deactivation of the catalyst. According to these authors the deactivation was explained by the physical blocking of pores by “green oil” and not by a poisoning of sites. The XPS and TPR results indicate that the active species on the surface of the alumina of the prepared catalysts is  $\text{WO}_3\text{-Al}_2\text{O}_3$ . The presence of  $\text{W}^{6+}$  species would favor the adsorption of the alkyne (two  $\pi$  bonds). Electrodeficient tungsten species would be responsible for the undesirable formation of “green oil” at a surface level, particularly at low reactions temperatures (293 and 303 K) but the additional influence of geometrical effects or the action of mixed sites cannot be disregarded. But the change in the reaction rate found for all the catalytic systems could also be related to a chemical equilibrium between the dissolved and surface reactants and products.

When the results obtained with catalysts of varying W concentration are analyzed the high activity of the 7.1WN/A catalyst, in comparison to that of 4.5WN/A or 8.5WN/A is notorious. 7.1% should be taken as the optimal load value for this kind of W catalysts prepared from ammonium metatungstate. Although the selectivity to (*Z*)-3-hexene is very high, its activity after 50 minutes of time-on-stream is not too high. This could be improved by preparing tungsten bimetallic catalysts. In previous reports of our group very good activity and selectivity values were obtained during the selective hydrogenation of 1-heptyne and 3-hexyne when using  $W_{2.4}-Pd_{0.4}$  bimetallic catalysts in which the W metal precursor was a phosphate one.<sup>15,53</sup> The higher activity of the bimetallic catalyst is related to an electronic effect originated by the superficial electron-rich species. In these reports deactivation was also observed at the lowest temperature (273 K). The high selectivity to (*Z*)-3-hexene found in the current work would indicate that the 7.1WN/A catalyst is a good material to be used as a base for the preparation of bimetallic W-Pd catalysts for selective hydrogenation of alkynes.

## CONCLUSIONS

Low cost tungsten catalysts were synthesized from ammonium metatungsten and alumina that proved to be active and selective for the hydrogenation of 3-hexyne, a non-terminal, medium length alkyne. The characterization by XRD, XPS and TPR revealed that the active species was  $WO_3-Al_2O_3$  (with  $W^{6+}$ ) on the alumina surface.

All the prepared catalysts proved to be active and selective to the (*Z*) isomer. The catalyst with 7.1 wt% W had the highest rate of conversion of 3-hexyne at all the studied reaction temperatures, 293, 303 and 323 K. In all the cases, regardless of the reaction temperature, the selectivity to the (*Z*)-alkene followed the order: 7.1WN/A > 8.5WN/A ≥ 4.5WN/A. There is a positive effect of the temperature on the reaction rate and on the selectivity. At 323 K a high selectivity of the 7.1WN/A catalyst to the (*Z*)-3-hexene was measured, ca. 94%, comparable to that obtained with the commercial Lindlar catalyst.

A change in the reaction rate of 3-hexyne was detected, starting at about 50 min of reaction time. Electrodeficient  $W^{6+}$  species would be responsible for the formation of green oil at the surface level, blocking pores and active sites of the catalyst, particularly at low reaction temperatures (293 and 303 K). But an equilibrium between the dissolved and surface reactant and products could not be discarded.

The performance of the catalysts can be interpreted in terms of electronic effects, related to the high charge of W (+6) causing an intensive dipole moment in the hydrogen molecule (van der Waals forces) conducting to a heterolytic bond rupture, then the generated  $H^+$  and  $H^-$  species approaching to the 3-hexyne alumina adsorbed molecule would provoke the heterolytic rupture of the  $C \equiv C$  into  $C^- = C^+$ . Low activities of 8.5WN/A could be explained by a steric effect related to the concentration of octahedral  $WO_3$ , that blocks the  $Al_2O_3$  support.

The high selectivity obtained is comparable to that of the classical and expensive Lindlar catalyst (5 wt% Pd) industrially used for this kind of reactions. The cheapest alumina supported tungsten catalysts could then be potential replacements of the Lindlar catalyst. To improve the mild activity found, the 7.1WN/A catalyst could be used to synthesize bimetallic W-Pd catalysts for selective hydrogenation of terminal and non-terminal alkynes.

## ACKNOWLEDGEMENTS

The financial support of UNL, CONICET and ANPCyT are greatly acknowledged.

## REFERENCES

1. Chinchilla, R.; Nájera, C.; *Chem. Rev.* **2014**, *114*, 1783.
2. Oger, C.; Balas, L.; Durand, T.; Galano, J.-M.; *Chem. Rev.* **2013**, *113*, 1313.
3. Ulan, J. G.; Wilhelm, F. M.; *J. Mol. Catal.* **1989**, *54*, 243.
4. McEwan, L.; Julius, M.; Roberts, S.; Fletcher, J. C. Q.; *Gold Bulletin* **2010**, *43*, 298.
5. Lindlar, H.; Dubuis, R.; Jones, F. N.; McKusick, B. C.; *Org. Synth.* **1966**, *46*, 89.
6. Liguori, F.; Barbaro, P.; *J. Catal.* **2014**, *311*, 212.
7. Ghosh, D.; Saravanan, S.; Gupta, N.; Abdi, S. H. R.; Khan, N. H.; Kureshy, R. I.; Bajaj, H. C.; *Asian J. Org. Chem.* **2014**, doi:10.1002/ajoc.201402130.
8. Choi, H.; Lee, E.; Jin, M.; Park, Y. K.; Kim, J. M.; Jeon, J. K.; *J. Nanosci. Nanotechnol.* **2014**, *11*, 8828.
9. Maccarrone, M. J.; Torres, G.; Lederhos, C.; Betti, C.; Badano, J. M.; Quiroga, M.; Yori, J.; In *Hydrogenation*; Karamé, I., ed.; InTech: Rijeka, **2012**, Chapter 7, pp 159-184.
10. Maccarrone, M. J.; Torres, G. C.; Lederhos, C.; Badano, J. M.; Vera, C. R.; Quiroga, M.; Yori, J. C.; *J. Chem. Technol. Biotechnol.* **2012**, *87*, 1521.
11. Mastalir, A.; Király, Z.; Patzko, A.; Dékány, I.; L'Argentiere, P.; *Carbon* **2008**, *46*, 1631.
12. Jung, A.; Jess, A.; Schubert, T.; Schütz, W.; *Appl. Catal., A* **2009**, *362*, 95.
13. Anderson, J. A.; Mellor, J. L.; Wells, R. P. K.; *J. Catal.* **2009**, *261*, 208.
14. Alvez-Manoli, G.; Pinnavaia, T. J.; Zhang, Z.; Lee, D. K.; Marín-Astorga, K.; Rodríguez, P.; Imbert, F.; Reyes, P.; Marín-Astorga, N.; *Appl. Catal. A* **2010**, *387*, 26.
15. Maccarrone, M. J.; Lederhos, C. R.; Torres, G.; Betti, C.; Coloma-Pascual, F. M.; Quiroga, E.; Yori, J. C.; *Appl. Catal. A* **2012**, *441*, 90.
16. Liprandi, D. A.; Cagnola, E. A.; Quiroga, M. E.; L'Argentiere, P. C.; *Catal. Lett.* **2009**, *128*, 423.
17. Liprandi, D. A.; Cagnola, E. A.; Paredes, J. F.; Badano, J. M.; Quiroga, M. E.; *Catal. Lett.* **2012**, *142*, 231.
18. Choi, J.; Yoon, N. M.; *Tetrahedron Lett.* **1996**, *37*, 1057.
19. Semagina, N.; Grasemann, M.; Xanthopoulos, N.; Renken, A.; Kiwi-Minsker, L.; *J. Catal.* **2007**, *251*, 213.
20. L'Argentiere, P. C.; Figoli, N. S.; *Ind. Eng. Chem. Res.* **1997**, *36*, 2543.
21. Lederhos, C. R.; Maccarrone, M. J.; Badano, J. M.; Coloma-Pascual, F.; Yori, J. C.; Quiroga, M. E.; *Appl. Catal., A* **2011**, *396*, 170.
22. Hong, Y.-K.; Lee, D.-W.; Eom, H.-J.; Lee, K.-Y.; *Appl. Catal., B* **2014**, *150*, 438.
23. Contreras, J. L.; Fuentes, G. A.; Zeifert, B.; Salmones, J.; *J. Alloys. Compd.* **2009**, *483*, 371.
24. Busto, M.; Benitez, V. M.; Vera, C. R.; Grau, J. M.; Yori, J. C.; *Appl. Catal., A* **2008**, *347*, 117.
25. Benitez, V. M.; Figoli, N. S.; *Catal. Commun.* **2002**, *3*, 487.
26. Nikulshina, P. A.; Minaeva, P. P.; Mozhaeva, A. V.; Maslakov, K. I.; Kulikovaa, M. S.; Pimerzina, A. A.; *Appl. Catal., B* **2015**, *176*, 374.
27. Huang, S.; Zhang, C.; He, H.; *Catal. Today* **2008**, *139*, 15.
28. Martín, C.; Solana, G.; Malet, P.; Rives, V.; *Catal. Today* **2003**, *78*, 365.
29. Cao, Y.; Wang, J.; Li, Q.; Yin, N.; Liu, Z.; Kang, M.; Zhu, Y.; *J. Fuel Chem. Technol.* **2013**, *41*, 943.
30. Chan, S.; Wachs, I.; Murrell, L.; Wang, L.; Hall, K.; *J. Phys. Chem.* **1984**, *88*, 5831.
31. NIST X-ray Photoelectron Spectroscopy Database NIST Standard Reference Database 20, Version 3.5 (Web Version), National Institute of Standards and Technology, USA, **2007**.
32. Benitez, V. M.; Querini, C. A.; Figoli, N. S.; Comelli, R. A.; *Appl. Catal., A* **1999**, *178*, 205.
33. Wang, C.; Lin H.; Ho, C.; *J. Mol. Catal. A: Chem.* **2002**, *180*, 285.

34. La Surface (web version) <http://www.lasurface.com/database/elementxps.php>, accessed in September 2015.
35. Elnashaie, S. S. E. H.; Elshishini, S. S.; *Modelling simulation and optimization of industrial fixed bed catalytic reactors*, Gorgon and Breach Science Publishers: **1993**, pp 398-400.
36. Sandelin, F.; Salmi, T.; Murzin, D.Y.; *Chem. Eng. Sci.* **2006**, *61*, 1157.
37. Salmi, T.; Murzin, D. Y.; Wärnä, J.; Mäki-Arvela, P.; Martin, G.; *Chem. Eng. Sci.* **2013**, *104*, 156.
38. Ahn, I. Y.; Lee, J. H.; Kun, S. S.; Moon, S. H.; *Catal. Today* **2007**, *123*, 151.
39. Ahn, I. Y.; Lee, J. H.; Kim, S. K.; Moon, S. H.; *Appl. Catal., A* **2009**, *360*, 38.
40. Wu, W.; Li, Y.-L.; Chen, W.-S.; Lai, C.-C.; *Ind. Eng. Chem. Res.* **2011**, *50*, 1264.
41. Pachulski, A.; Schödela, R.; Claus, P.; *Appl. Catal., A* **2011**, *400*, 14.
42. Pachulski, A.; Schödela, R.; Claus, P.; *Appl. Catal., A* **2012**, *445*, 107.
43. Kolli, N.; Delannoy, L.; Louis, C.; *J. Catal.* **2013**, *297*, 79.
44. Bartholomew, C. H.; *Appl. Catal., A* **2001**, *212*, 17.
45. Blackmond, D. G.; Goodwin, J. G.; Lester, J. E.; *J. Catal.* **1982**, *78*, 34.
46. Karge, H. G.; *Stud. Surf. Sci. Catal.* **1991**, *58*, 531.
47. Gamas, E. D.; Schifter, I.; *Stud. Surf. Sci. Catal.* **1997**, *111*, 119.
48. Bai, J.; Liu, S. L.; Xie, S. J.; Xu, L. Y.; Lin, L. W.; *Stud. Surf. Sci. Catal.* **2004**, *147*, 715.
49. Fajula, F.; Gault, F. G.; *J. Catal.* **1981**, *68*, 312.
50. Langner, B. E.; Meyer, S.; *Stud. Surf. Sci. Catal.* **1980**, *6*, 91.
51. Karge, H. G.; Boldingh, E. P.; *Catal Today* **1988**, *3*, 53.
52. Esmaili, E.; Rashidi, A. M.; Mortazavi, Y.; Khodadadi, A. A.; Rashidzadeh, M.; *J. Energy Chem.* **2013**, *22*, 717.
53. Lederhos, C. R.; Badano, J. M.; Quiroga, M. E.; Coloma-Pascual, F.; L'Argentièrre, P. C.; *Quim. Nova*, **2010**, *33*, 816.